



This is a repository copy of *Magnitude-sensitive reaction times reveal non-linear time costs in multi-alternative decision-making*.

White Rose Research Online URL for this paper:  
<https://eprints.whiterose.ac.uk/184024/>

Version: Submitted Version

---

**Article:**

Marshall, J.A.R. [orcid.org/0000-0002-1506-167X](https://orcid.org/0000-0002-1506-167X), Reina, A. [orcid.org/0000-0003-4745-992X](https://orcid.org/0000-0003-4745-992X), Hay, C. et al. (2 more authors) (Submitted: 2021) Magnitude-sensitive reaction times reveal non-linear time costs in multi-alternative decision-making. bioRxiv. (Submitted)

<https://doi.org/10.1101/2021.05.05.442775>

---

**Reuse**

This article is distributed under the terms of the Creative Commons Attribution (CC BY) licence. This licence allows you to distribute, remix, tweak, and build upon the work, even commercially, as long as you credit the authors for the original work. More information and the full terms of the licence here:  
<https://creativecommons.org/licenses/>

**Takedown**

If you consider content in White Rose Research Online to be in breach of UK law, please notify us by emailing [eprints@whiterose.ac.uk](mailto:eprints@whiterose.ac.uk) including the URL of the record and the reason for the withdrawal request.



[eprints@whiterose.ac.uk](mailto:eprints@whiterose.ac.uk)  
<https://eprints.whiterose.ac.uk/>

# 1 Magnitude-sensitive reaction times 2 reveal non-linear time costs in 3 multi-alternative decision-making

4 **James A. R. Marshall**<sup>1\*</sup>, **Andreagiovanni Reina**<sup>1,2</sup>, **Célia Hay**<sup>3</sup>, **Audrey Dussutour**<sup>3</sup>,  
5 **Angelo Pirrone**<sup>4</sup>

\*For correspondence:

[james.marshall@sheffield.ac.uk](mailto:james.marshall@sheffield.ac.uk)  
(JARM)

6 <sup>1</sup>Department of Computer Science, University of Sheffield, UK; <sup>2</sup>IRIDIA, Université Libre  
7 de Bruxelles, Belgium; <sup>3</sup>Research Centre for Animal Cognition (CRCA), Centre for  
8 Integrative Biology (CBI), Toulouse University, France; <sup>4</sup>Centre for Philosophy of Natural  
9 and Social Science, London School of Economics and Political Science, UK

## 10 Abstract

11 Optimality analysis of value-based decisions in binary and multi-alternative choice settings predicts  
12 that reaction times should be sensitive only to differences in stimulus magnitudes, but not to overall  
13 absolute stimulus magnitude. Yet experimental work in the binary case has shown magnitude  
14 sensitive reaction times, and theory shows that this can be explained by switching from linear  
15 to geometric time costs, but also by nonlinear subjective utility. Thus disentangling explanations  
16 for observed magnitude sensitive reaction times is difficult. Here for the first time we extend the  
17 theoretical analysis of geometric time-discounting to ternary choices, and present novel experi-  
18 mental evidence for magnitude-sensitivity in such decisions, in both humans and slime moulds.  
19 We consider the optimal policies for all possible combinations of linear and geometric time costs,  
20 and linear and nonlinear utility; interestingly, geometric discounting emerges as the predominant  
21 explanation for magnitude sensitivity.

## 22 Introduction

23 While the normative, optimal policy, approach to understanding decision-making is now well  
24 established for perceptual decisions (e.g. *Bogacz et al. (2006)*), it has only recently been applied to  
25 value-based decisions (*Fudenberg et al., 2018; Tajima et al., 2016, 2019*); such decisions differ from  
26 perceptual decisions because decision makers are rewarded by the value of the selected option,  
27 rather than whether or not they selected the best option (e.g. *Pirrone et al. (2014); Tajima et al.*  
28 *(2016, 2019); Krajbich et al. (2010)*). Recently researchers have analysed multi-alternative value-  
29 based decision-making (*Tajima et al., 2019*), building on earlier work in optimal decision policies

30 for binary value-based choices (*Tajima et al., 2016*). Through sophisticated analysis based on the  
31 standard tool for solving such decision problems, stochastic dynamic programming (*Mangel and*  
32 *Clark, 1988; Houston and McNamara, 1999*), the authors also present neurally-plausible decision  
33 mechanisms that may implement or approximate the optimal decision policies (*Tajima et al.,*  
34 *2016, 2019*). These policies turn out to be described by rather simple and well-known decision  
35 mechanisms, such as drift-diffusion models with decision thresholds that collapse over time for the  
36 binary case (*Tajima et al., 2016*), and nonlinear time-varying thresholds that interpolate between  
37 best-vs-average and best-vs-next in the multi-alternative case (*Tajima et al., 2019*).

38 Interestingly, the theoretically optimal policy for the binary decision case (*Tajima et al., 2016*) is  
39 inconsistent with empirical observations of magnitude-sensitive reaction-times (*Teodorescu et al.*  
40 *(2016); Pirrone et al. (2018a); Steverson et al. (2019); Zajkowski et al. (2019); Turner et al. (2019),*  
41 *but see Bhui (2019)*), unless assumptions are made that subjective utilities for decision-makers  
42 are nonlinear, or decisions are embedded in a fixed-length time period with known or learnable  
43 distributions of trial option values, so that a variable opportunity cost arises from decision time  
44 (*Tajima et al., 2016*). Furthermore, even single-trial dynamics lead to magnitude sensitive reaction  
45 times (*Pirrone et al., 2018b*).

46 Previous analyses made an assumption that appears widespread in psychology and neuro-  
47 science, that decision-makers should optimise their Bayes Risk from such decisions (*Tajima et al.,*  
48 *2016, 2019*); this is equivalent to maximising the expected value of decisions in which there is a  
49 linear cost for the time spent deciding (*Bogacz et al., 2006; Pirrone et al., 2014*). For a lab subject in  
50 a pre-defined and known experimental design this may appear appropriate, for example because  
51 there may be a fixed time duration within which a number of decision trials will occur and the  
52 subject can learn the value distribution of the trials (e.g. *Bogacz et al. (2006); Pirrone et al. (2014)*).  
53 However, an alternative and standard formulation of the Bellman equation, the central equation  
54 in constructing a dynamic program, accounts for the cost of time by discounting future rewards  
55 geometrically, so a reward one time step in the future is discounted by rate  $\gamma < 1$ , two time steps  
56 in the future by  $\gamma^2$ , and so on (see Materials and Methods). This is a standard assumption in  
57 behavioural ecology (*Mangel and Clark, 1988; Houston and McNamara, 1999*), in which discount-  
58 ing the future means that future rewards are not guaranteed but are uncertain, due to factors  
59 such as interruption, consumption of a food item by a competitor, mortality, and so on. Thus  
60 discounting the future represents the inherent uncertainty that animals must make decisions  
61 under in their natural environments, in which their brains evolved. The appropriate discount is  
62 then the probability that future rewards are realised, hence geometric discounting is optimal since  
63 probabilities multiply. Indeed there is extensive evidence of such reward discounting in humans  
64 and other animals (e.g. *Sellitto et al. (2010)*, although this frequently suggests hyperbolic rather  
65 than geometric discounting, a fact that in itself merits an explanation based on optimality theory  
66 (*McNamara and Houston, 2009*)).

67 Rederiving optimal policies to account for geometric (*Marshall, 2019*) or general multiplicative  
68 (*Steverson et al., 2019*) costs of time qualitatively changes them in the binary decision case, in-  
69 troducing magnitude-sensitive reaction times (*Marshall, 2019; Steverson et al., 2019*). However,  
70 disentangling these from nonlinear subjective utility is challenging, and cannot be excluded as  
71 an explanation for previous results (*Teodorescu et al., 2016; Pirrone et al., 2018a; Steverson et al.,*  
72 *2019; Zajkowski et al., 2019; Turner et al., 2019; Bhui, 2019; Smith and Krajbich, 2019; Pirrone and*  
73 *Gobet, 2021*).

74 Here for the first time we extend the theoretical and experimental study of magnitude-sensitivity  
75 to three-alternative decisions. We first present evidence for magnitude-sensitive reaction times in  
76 three-way equal-alternative decisions. We then present optimal policy analyses and novel numerical  
77 simulations for such ternary decisions, both in human subjects undertaking a psychophysical task,  
78 and unicellular organisms engaged in foraging. Importantly, for a wide variety of utility functions,  
79 strong magnitude-sensitivity is only observed when there is a multiplicative cost for time, rather  
80 than the previously assumed linear time cost. Thus magnitude-sensitivity is revealed as genuinely  
81 diagnostic for multiplicative time costing, as all other assumptions either do not generate this  
82 phenomenon, or can be discounted.

## 83 Results

84 As we were testing theory developed to explain decision-making by animals with brains, we con-  
85 ducted psychophysical experiments with human subjects. However, we also conducted foraging  
86 experiments with a unicellular slime mould; testing theory across multiple species and behavioural  
87 tasks increases confidence when multiple agreements with theory are observed (*Pirrone et al.,*  
88 *2018a*), and slime moulds have become a model system, with multiple experiments seeking to  
89 reproduce behavioural predictions from neuroscience and psychology (*Latty and Beekman, 2011;*  
90 *Reid et al., 2016; Dussutour et al., 2019*).

91 Multi-Alternative Decisions in Human Psychophysical Trials are Magnitude-Sensitive  
92 Here we provide strong empirical evidence for magnitude sensitivity with multiple alternatives in  
93 humans, using an experimental paradigm similar to the one used to show magnitude sensitivity  
94 for two-alternative decision making (*Teodorescu et al., 2016; Pirrone et al., 2018a*). Details of the  
95 experiment (methods, participants, etc.) are reported in Materials and Methods. Participants had to  
96 choose which of three above-threshold grey patches was brighter in an online experiment. Although  
97 the experiment included conditions for which a brighter alternative existed, conditions of interest  
98 were equal alternatives of different magnitude, that is, conditions for which the three patches had  
99 the same brightness that could vary across magnitude conditions. Equal alternatives allow us to test  
100 hypotheses regarding magnitude sensitivity, by keeping differences in evidence constant (*Pirrone*  
101 *et al., 2018a,b; Pirrone and Gobet, 2021*).

102 As previously done for binary decisions (*Pirrone et al., 2018a,b*), here we focused our analyses  
103 exclusively on equal alternatives. For the analyses, we did not censor any datapoints.

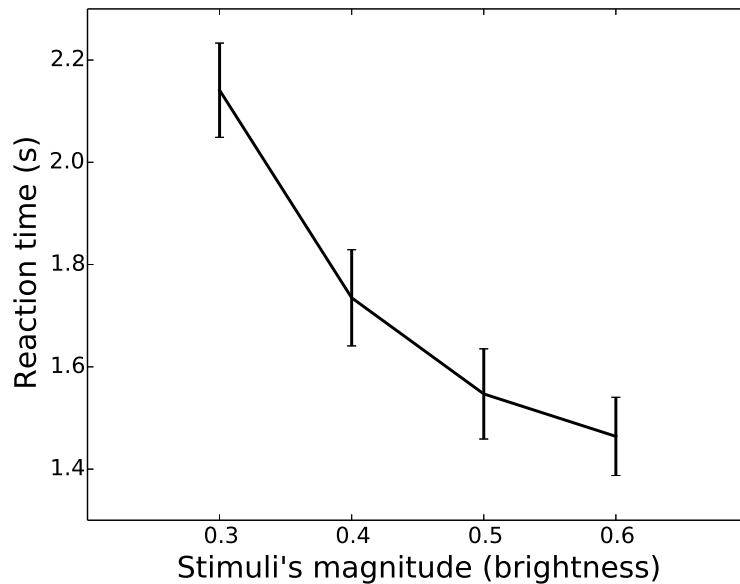


**Figure 1.** Empirical results from the behavioural online experiment. Decreasing reaction times as a function of the magnitude of the equal alternatives. X-axis presents mean brightness of equal alternatives (0.3, 0.4, 0.5, 0.6), on a scale of brightness from 0 to 1 in PsychoPy. Y-axis presents mean reaction times, in seconds. Bars show 95% confidence intervals. Participants experienced equal alternative conditions, interleaved with unequal alternative trials in pseudo-randomised order. Participants that performed the whole experiment experienced each equal alternative presentation ten times.

104 As shown in Figure 1, the data show strong magnitude sensitivity, given that choices for equal  
105 alternatives of higher magnitude conditions (higher brightness on a scale from 0 to 1 on Python)  
106 were made faster.

107 To assess if reaction times decreased as a function of the mean brightness of the equal al-  
108 ternatives, we used a linear mixed model in R. The model was fitted by specifying as fixed effect  
109 (explanatory variable) the brightness of equal alternatives as a continuous predictor. The partici-  
110 pant ID was also added to the model as a factor for random effects. Reaction times significantly  
111 decreased as a function of the mean brightness of the alternatives ( $b = -1.95$ ,  $p < .001$ , CI -2.14 -1.75).  
112 Further details for the mixed-effect regression are presented in the supplementary information  
113 (Table S1).

114 As the COVID-19 pandemic necessitated an online experiment we could not collect or control  
115 information on a number of possible confounds (viewer position, motivation, room luminosity, etc.),  
116 and there are multiple sources of unaccounted variability in our online experiment; however there  
117 is no *a priori* reason to expect these to act as consistent confounds in the magnitude-sensitive  
118 reaction times observed. Furthermore, the very large sample size for our study ( $N = 117$ ; compared  
119 to  $N = 8$  and  $N = 9$  for previous similar investigations (*Teodorescu et al., 2016; Pirrone et al.,*  
120 *2018a*)) should minimise effects due to randomly-distributed confounds.

121 Multi-Alternative Decisions in Foraging Trials by Unicellular Organisms are Magnitude-  
122 Sensitive

123 Here, using slime moulds of the species *Physarum polycephalum*, we also observed strong empirical  
124 evidence for magnitude sensitivity with three alternative foraging tasks. Details of the experiment  
125 are reported in Materials and Methods. Slime moulds were confronted with a choice offering three  
126 equal food sources. We increased the magnitude of the options by increasing the quality of the food  
127 sources. As shown in Figure 2, the latency to reach one of the alternatives depends on the quality of  
128 the food sources; the higher the quality the faster the slime mould. This was confirmed by a linear  
129 mixed model similar to the one applied to the human data, in which reaction times significantly  
130 decreased as a function of food quality ( $b = -0.03$ ,  $p < .001$ , CI  $-0.03$   $-0.02$ ; further details, Table S2 in  
131 the supplementary information).

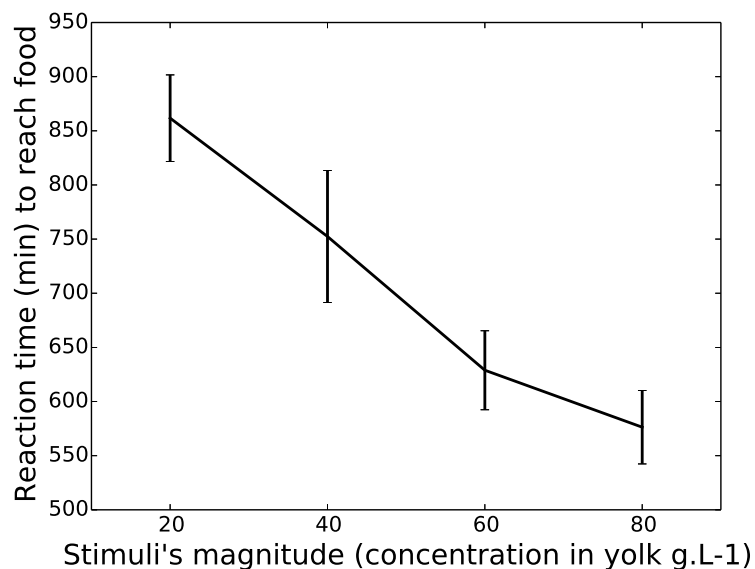


**Figure 2.** Empirical results from the slime mould experiment. Decreasing latencies to reach a food source as a function of the magnitude of the equal alternatives. X-axis presents the concentration in egg yolk of equal food sources (20, 40, 60, 80 g.L-1). Y-axis presents mean latency to reach a food source, in minutes. Bars show 95% confidence intervals. 50 slime moulds were tested for each magnitude for a total of 200 slime moulds.

132 **Optimal Policies**

133 For our theoretical analysis we begin by re-deriving optimal policies for decisions when the change  
134 is made from linear costing of time, or Bayes Risk, to geometric discounting of future reward. Note  
135 that geometric discounting of future rewards is similar to, but not the same as, non-linear utility. As  
136 remarked in the introduction above, for binary decisions magnitude-sensitive reaction times can be  
137 explained by optimal decision policies for either multiplicative (e.g. geometric) time discounting  
138 (*Marshall, 2019; Steverson et al., 2019*) or nonlinear subjective utility with linear time costs (*Tajima*  
139 *et al., 2016*). In the multi-alternative case, on the other hand, the picture is more nuanced; moving  
140 from linear costing of time to geometric discounting of future rewards changes complicated time-

141 dependent non-linear decision thresholds ((*Tajima et al., 2019*) Fig. 7) into either simple linear ones  
 142 that collapse over time for lower-value option sets (Fig. 3), or nonlinear boundaries that evolve  
 143 over time similarly to the Bayes Risk-optimising case for higher-value option sets (*Marshall (2019)*;  
 144 Fig. 3). As *Tajima et al.* note, the simpler linear decision boundaries implement the ‘best-vs-average’  
 145 decision strategy, whereas the more complex boundaries interpolate between ‘best-vs-average’  
 146 and ‘best-vs-next’ decision strategies (*Tajima et al., 2019*); interestingly simply moving to nonlinear  
 147 subjective utility with linear time costs simplifies the decision strategy to the ‘best-vs-next’ strategy  
 148 (Fig. 3; see *Tajima et al. (2019)*, Fig. 6C).

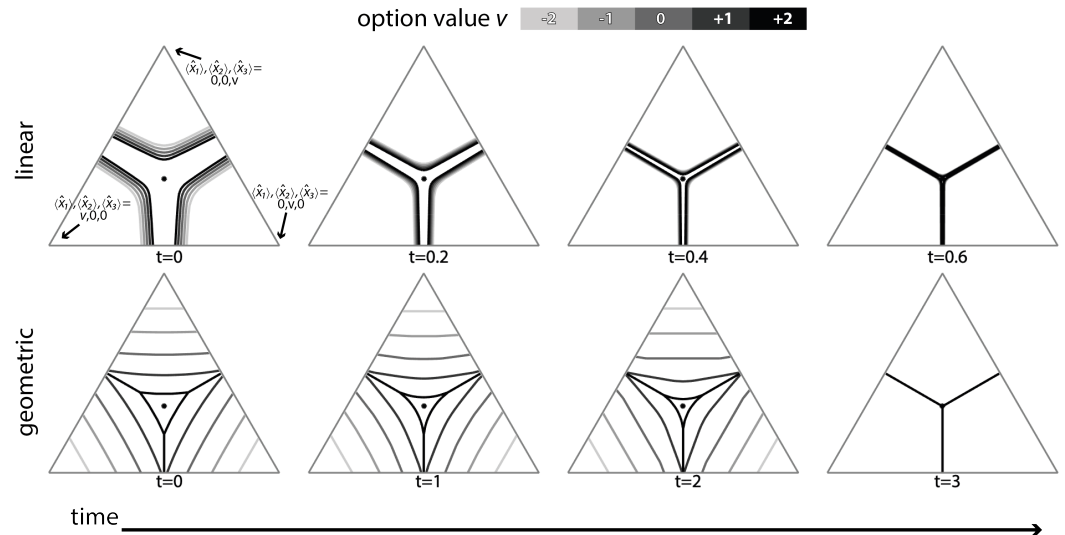


**Figure 3.** Linear time costs lead to weakly magnitude-sensitive optimal policies (top row), while geometric discounting of reward leads to strongly magnitude-sensitive optimal policies (bottom row). In the linear time cost (Bayes Risk) case nonlinear subjective utility changes complex time and value-dependent decision boundaries in estimate space into a simple mostly magnitude-insensitive ‘best-vs-next’ strategy (top row; see *Tajima et al. (2019)*, Fig. 6C). For geometric discounting of rewards over time, optimal decision boundaries are strongly magnitude-sensitive and interpolate between simple ‘best-vs-average’ and ‘best-vs-next’ strategies (see *Tajima et al. (2019)*, Fig. 6). Triangles are low dimensional projections of the 3-dimensional evidence estimate space onto a plane moving along the equal value line, at value  $v$  (*Tajima et al., 2019*). Dynamic programming parameters were: prior mean  $\bar{x}_{p,i} = 1.5$  and variance  $\sigma_{p,i}^2 = 5$ , waiting time  $t_w = 1$ , temporal costs  $c = 0$ ,  $\gamma = 0.2$ , and utility function parameters  $m = 4, s = 0.25$  (for the linear time cost) and  $m = 4, s = 3.5$  (for the geometric time cost).

149 Multi-Alternative Decisions: Optimal Policies are Weakly Magnitude-Sensitive for Nonlin-  
 150 ear Subjective Utility Under Bayes Risk-Optimisation

151 Under Bayes Risk-optimisation it is known that, for binary decisions, optimal policies are magni-  
 152 tude-insensitive when subjective utility is linear, whereas they are magnitude-sensitive when subjective  
 153 utility is nonlinear (*Tajima et al., 2016, 2019*).

154 For ternary decisions, however, even with nonlinear subjective utility, policies exhibit very weak  
 155 magnitude-sensitivity early in decisions, becoming magnitude-insensitive as decisions progress  
 156 (Fig. 3, row ‘linear’). Sensitivity analysis shows that magnitude-insensitivity is a general pattern. An  
 157 informal understanding of this can be arrived at by appreciating that sigmoidal functions have

158 two extremes of parameterisation; in one extreme they are almost linear, hence will be mostly  
 159 magnitude insensitive due to the known result (*Tajima et al., 2016*). At the other extreme, the  
 160 function becomes step-like; in this case options are either good or bad, and the optimal policy  
 161 rapidly becomes 'choose the best' (Fig. 4), since under such a scenario sampling is of minimal benefit  
 162 as early information quickly indicates whether an option is good or bad, and choosing the first  
 163 option that appears to be good is optimal.

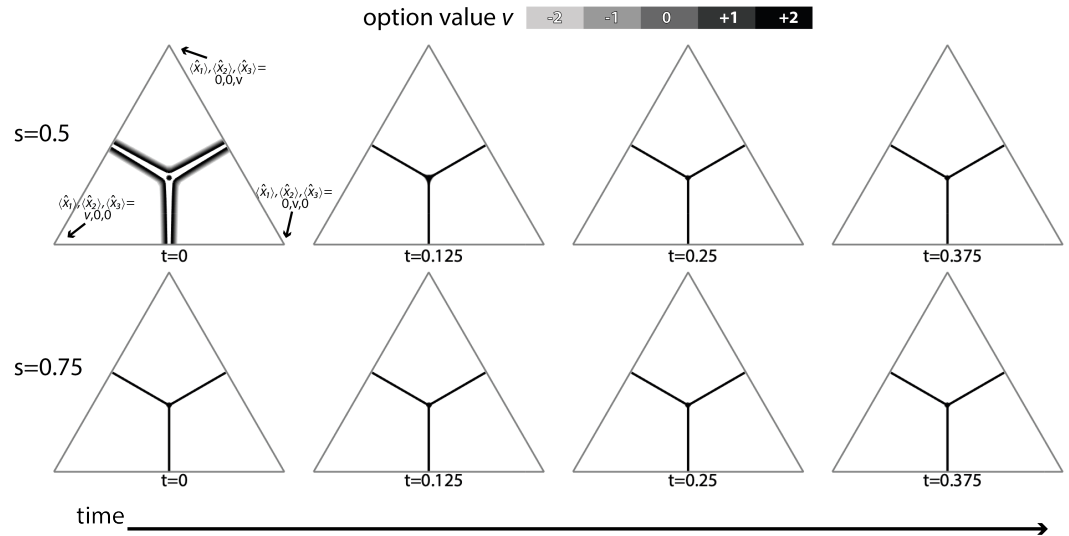


**Figure 4.** Optimal policies for linear time cost (Bayes Risk) rapidly transition from approximately linear subjective utility, and hence weakly magnitude-sensitive, decision boundaries in estimate space (Fig. 3, top row for  $s = 0.25$ ; present figure, top row for  $s = 0.5$ , to more step-like subjective utility where immediate 'choose the best' decision-boundaries are necessarily magnitude-insensitive (bottom row for  $s = 0.75$ , and higher values of  $s$ ). Triangles are low dimensional projections of the 3-dimensional evidence estimate space onto a plane moving along the equal value line, at value  $v$  (*Tajima et al., 2019*). Dynamic programming parameters were: prior mean  $\bar{x}_{p,i} = 1.5$  and variance  $\sigma_{p,i}^2 = 5$ , and utility function parameters  $m = 4$ ,  $s \in \{0.5, 0.75\}$ .

164 Multi-Alternative Decisions: Optimal Policies Become Magnitude-Sensitive Under Geo-  
 165 metric Discounting

166 As previously shown (*Marshall, 2019; Steverson et al., 2019*), assuming geometric temporal dis-  
 167 counting, the optimal policy for binary decisions is magnitude-sensitive. In ternary decisions,  
 168 geometric discounting has the same effect; regardless of utility function linearity, the optimal policy  
 169 is magnitude-sensitive (Fig. 3, row 'geometric').

## 170 Numerical Simulations

171 Since noise-processing is fundamental in determining reaction times, we confirmed the results on  
 172 magnitude sensitivity from our optimal policy analysis via numerical simulation of Bayes-optimal  
 173 evidence-accumulating agents using those policies (see Materials and Methods). These numerical  
 174 simulations confirmed the qualitative results from the optimal policy analysis; reaction times for  
 175 ternary decisions under linear time costing are only weakly magnitude sensitive even for nonlinear



176 subjective utility functions, while under geometric time costing reaction times become strongly  
 177 magnitude sensitive for most utility functions examined.

178 Multi-Alternative Decisions: Simulated Reaction Times are Weakly Magnitude-Sensitive  
 179 for Nonlinear Subjective Utility Under Bayes Risk-Optimisation

180 Across all nonlinear subjective utility functions considered, linear time costing resulted in weakly  
 181 magnitude-sensitive simulated reaction times (Fig. 5). This agrees with the weak magnitude-  
 182 sensitivity observed in the optimal policies derived above (Fig. 3). Note, however, that this contrasts  
 183 with the binary decision case in which optimal policies, and hence reaction times, become magnitude  
 184 sensitive under linear time cost when subjective utility is nonlinear (*Tajima et al., 2016*). An informal  
 185 justification for this is given above in analysis the optimal decision boundaries computed via  
 186 dynamic programming.

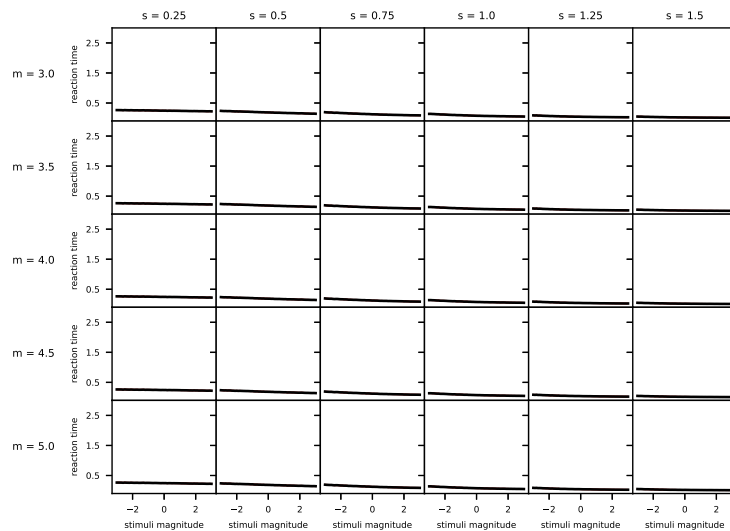


**Figure 5.** Linear time costs lead to weakly magnitude-sensitive simulated reaction times across a range of nonlinear subjective utility functions for equal value option sets. Simulation parameters were: prior mean  $\bar{x}_{p,i} = 1.5$  and variance  $\sigma_{p,i}^2 = 5$ , observation noise variance  $\sigma_{a,i}^2 = 2$ , temporal cost  $c = 0$ , waiting time  $t_w = 1$ , and simulation timestep  $dt = 5 \times 10^{-3}$ . Lines are the mean reaction time for  $10^4$  simulations, 95% confidence intervals are shown as red shading (mostly invisible because smaller than the linewidth).

187 Multi-Alternative Decisions: Simulated Reaction Times Become Magnitude-Sensitive Un-  
 188 der Geometric Discounting

189 In contrast to linear time costing, across all nonlinear subjective utility functions considered, ge-  
 190 ometric time costing resulted in strongly magnitude sensitive simulated reaction times (Fig. 6),  
 191 with longer reaction times for lower value equal-value option sets; this strategy was previously  
 192 hypothesised to be optimal (*Pais et al., 2013*). The strong magnitude-sensitivity in the numerical  
 193 simulations corresponds with the strong magnitude-sensitivity observed in the optimal policies  
 194 derived above (Fig. 3).

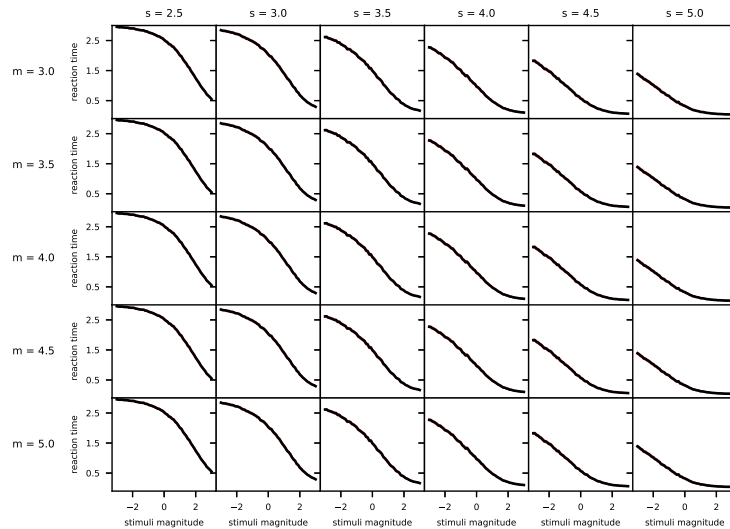


**Figure 6.** Geometric discounting of reward leads to strongly magnitude-sensitive simulated reaction times across a range of nonlinear subjective utility functions, with decisions postponed for low equal-value option sets. Simulation parameters were: prior mean  $\bar{x}_{p,i} = 1.5$  and variance  $\sigma_{p,i}^2 = 5$ , observation noise variance  $\sigma_{a,i}^2 = 2$ , temporal cost  $\gamma = 0.1$ , and simulation timestep  $dt = 5 \times 10^{-3}$ . Lines are the mean reaction time for  $10^4$  simulations, 95% confidence intervals are shown as red shading (mostly invisible because smaller than the linewidth).

---

## 195 Discussion

196 In understanding behaviour, which is a product of evolution, searching for optimal algorithms for  
197 typical decision problems can provide great insight. This normative approach can explain observed  
198 behaviours, and predict new behavioural patterns, based on evolutionary advantage. Yet the  
199 assumptions underlying such model analyses can prove crucial. Recently it has been asked what  
200 optimal decision algorithms look like for multi-alternative value-based choices, in which subjects are  
201 rewarded not by whether their decision was correct or not, but by the value to them of the selected  
202 option (*Tajima et al., 2019*). The resulting algorithms correspond to earlier simple models for  
203 perceptual and value-based decision-making. These findings, however, rest on an assumption that  
204 time is a linear cost for subjects. Here we have shown that deciding human subjects and foraging  
205 unicellular organisms do, however, exhibit marked magnitude sensitivity in ternary decisions, as  
206 previously shown for binary decisions (*Pirrone et al., 2018a; Dussutour et al., 2019*). We have also  
207 shown that optimality theory that discounts future rewards multiplicatively based on time is the  
208 foremost explanation for such observations of magnitude-sensitivity; nonlinear subjective utility  
209 alone is not sufficient to give rise to strongly magnitude-sensitive decision times when time is  
210 treated as a linear cost.

## 211 Behavioural Predictions

212 The Bayes Risk optimal policy is approximated by a neural model that is consistent with observations  
213 of economic irrationality (*Tajima et al., 2019*), hence it will be important to see if a revised neural

214 model based on the revised optimal policy still shows such agreement. For example, while in the  
215 binary case magnitude-sensitive reaction times can be explained both by nonlinear subjective utility  
216 functions, and by multiplicative discounting rather than Bayes Risk, in the multi-alternative case our  
217 analysis suggests that the same phenomenon is explained *primarily* by multiplicative discounting of  
218 future rewards and not by nonlinear utility.

## 219 **Optimality Criteria**

220 Practitioners of behavioural ecology have established principles to deal with empirically-observed  
221 deviations from the predictions of optimality theory (*Parker and Smith, 1990*); two of the most  
222 useful are to consider that the optimisation criterion has been misidentified, or the behaviour in  
223 question is not really adaptive. Tajima and colleagues employ an exemplary approach, attempting  
224 to combine the best of the approaches of normative and mechanistic modelling (*McNamara and*  
225 *Houston, 2009*); yet it bears remembering that subjects may not be trying optimally to solve the  
226 simple decision problem they are presented in the lab, but rather making use of mechanisms that  
227 evolved to solve the problem of living in their natural environment (*Fawcett et al., 2014*); indeed  
228 the experimental data presented here were produced by subjects who received no reward, yet  
229 nevertheless acted as if they were making an economic, value-based, decision rather than a purely  
230 perceptual, accuracy-based one.

## 231 **Materials and Methods**

### 232 **Psychophysical Experiment**

#### 233 **Participants**

234 This experiment was conducted during the COVID-19 pandemic, from May 13th – June 1st 2020..  
235 Given that it was not possible to recruit participants for a laboratory experiment, we instead  
236 recruited them online using Pavlovia (*Peirce et al., 2019; Peirce, 2007*), an online platform for  
237 psychophysical experiments implemented in PsychoPy.

238 Running a perceptual experiment online has a number of limitations: first, there is no way to  
239 ensure that participants are focused on the task and minimising distractions - to mitigate this we  
240 kept the task short and participants were instructed to concentrate on it; second, Pavlovia (as of  
241 March-May 2020) only allows stimuli to be drawn in units relative to window size (i.e., the window in  
242 which the experiment is displayed) or in pixels, hence their size and position relative to the fixation  
243 cross will vary across devices, depending on specific window sizes. However, even if the size and  
244 location of stimuli could be kept constant across participants, participants' distance from the screen  
245 cannot be controlled during an online experiment.

246 While in previous two-alternative experiments (*Teodorescu et al., 2016; Pirrone et al., 2018a*)  
247 a limited number of participants ( $N < 10$ ) performed a large number of trials, for our online  
248 experiment we aimed at a large number of participants performing a limited number of trials.

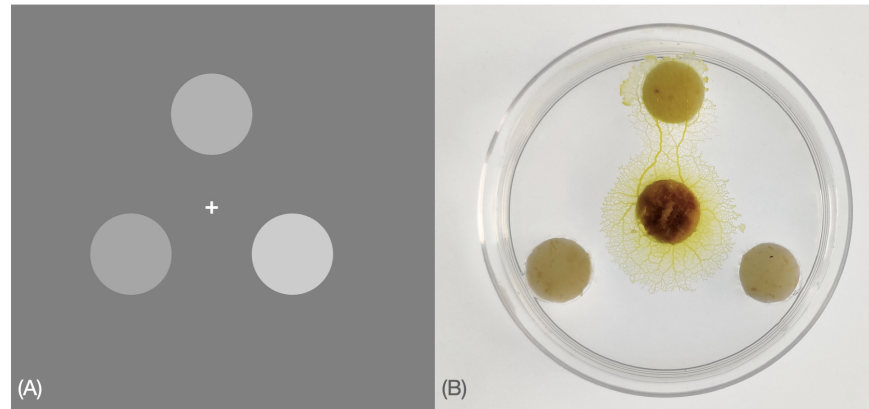


**Figure 7.** (A) Stimuli example for human psychophysical experiments: Participants were requested to decide as fast and accurately as possible which of the three stimuli was brighter; they were asked to maintain fixation on the cross at the centre of the screen and minimise distraction for the short duration of the experiment. Unknown to participants, conditions of interest were conditions for which the stimuli had equal mean brightness. (B) Photograph showing a slime mould that chose one food alternative among three equal ones. The slime mould was placed in the centre of a petri dish (6cm  $\varnothing$ ) filled with agar gel (10 g/l) at a distance of 2cm from each food alternative.

249 This strategy is beneficial for online studies since the large number of participants helps ensure  
250 that variation in participants' motivation or viewing arrangements is averaged out. We therefore  
251 recruited 117 participants via external advertisement on Twitter, and internal email lists at the  
252 University of Sheffield (mean age = 40.4, SD = 11.2774, range 23 -77; 79 females, 37 males, 1 did  
253 not indicate their gender). We requested participants to follow the link to the experiment only if  
254 aged 18 years or older. The experiment lasted about 5 minutes and participation was voluntary;  
255 participants did not receive any reward for their participation.

256 After reading the instructions, participants were informed that by continuing they were confirm-  
257 ing that they understood the nature of the experiment and consented to participate. Participants  
258 were also informed that they could leave the experiment at any time by closing the browser. For this  
259 experiment, all procedures were approved by the University of Sheffield, Department of Computer  
260 Science Ethics Committee.

### 261 **Experimental setup**

262 Similarly to previous studies (*Teodorescu et al., 2016; Pirrone et al., 2018a*), stimuli consisted of  
263 three homogeneous, round, white patches in a triangular arrangement on a grey background, as  
264 depicted in Figure 7. Throughout the task participants were presented with a central fixation cross  
265 that they were requested to fixate on.

266 On a scale from 0 to 1 in PsychoPy, the patches could have a brightness of 0.3, 0.4, 0.5 or 0.6.  
267 There were  $4^3 = 64$  possible trial combinations, of which 4 were equal alternatives (i.e., alternatives  
268 having a brightness of [0.3,0.3,0.3], [0.4,0.4,0.4], [0.5,0.5,0.5] or [0.6,0.6,0.6]). We selected 10 equal  
269 trial repeats, and only one trial repeat for all possible unequal alternatives, for a total of 100

270 trials per participant. On each frame, a Gaussian random variable with mean 0 and standard  
271 deviation of  $0.25 \times$  (mean brightness of the alternative) was added separately to the brightness  
272 level of each patch; the signal-to-noise ratio was thus kept constant across equal alternatives of  
273 different magnitude. The order of presentation of the alternatives was pseudo-randomised across  
274 participants and there was no systematic link between patch position and best option.

275 Three grey patches were presented simultaneously on the screen and subjects were asked to  
276 decide which of the three was brighter by pressing 'left', 'right' or 'up' on a keyboard using their  
277 second, fourth or third right-hand fingers, via a line-drawn diagram of a hand over a keyboard  
278 presented before the experiment began; specific instructions for left-handed participants were not  
279 provided, and we did not record handedness. The inter-trial interval, during which participants  
280 were presented with only the fixation cross, was selected at random between 0.5 seconds, 1 second  
281 or 1.5 seconds for each trial. Subjects were instructed to be as fast and accurate as possible and to  
282 maintain their fixation on the cross at the centre of the screen throughout the experiment. Before  
283 the experiment they were presented with 6 training trials (unequal alternatives) to familiarise  
284 themselves with the task. Participants were not provided with any feedback after each trial and  
285 were not informed about the presence of the equal-alternatives conditions.

## 286 **Slime Mould Experiment**

287 *Physarum polycephalum*, also known as the acellular slime mould, is a giant polynucleated single cell  
288 organism that inhabits shady, cool, and moist areas. In the wild, *P. polycephalum* eats bacteria and  
289 dead organic matter. In the presence of chemical stimuli in the environment, slime moulds show  
290 directional movements (*i.e.* chemotaxis).

291 Slime moulds of strain LU352 kindly provided by Professor Dr Wolfgang Marwan (Max Planck  
292 Institute for Dynamics of Complex Technical Systems, Magdeburg, Germany) were used for the  
293 experiments. Slime moulds were initiated with a total of 10 sclerotia which are encysted resting  
294 stages. The sclerotia were soaked in water and placed in petri dishes (140 mm  $\varnothing$ ) on agar gel  
295 (1%). Once revived, slime moulds start to explore the agar gel, usually 24h after the reactivation of  
296 the sclerotia. The slime moulds were then reared for a month on a 1% agar medium with rolled  
297 oat flakes (Quaker Oats Company®) in Petri dishes (140 mm  $\varnothing$ ). They were kept in the dark in a  
298 thermoregulated chamber at a temperature of 20 degrees Celsius and a humidity of 80%. The day  
299 before the experiment the slime moulds were transferred on a 10% oat medium (powdered oat  
300 in a 1% agar solution) in Petri dishes (diameter 140 mm). The experiments were carried out in a  
301 thermoregulated chamber and pictures were taken with a Canon 70D digital camera.

302 Slime moulds were presented with a choice between three equal food sources in an arena  
303 consisting of 60 mm diameter Petri dish filled with plain 1% agar. We punched three holes (10mm  
304  $\varnothing$ ) in the arena and filled them with a food source (10mm  $\varnothing$ ). We used four different food patches  
305 varying in quality: 2% w/v powdered oat mixed with either 2, 4, 6 or 8% w/v egg yolk. Once the

306 food sources were set in each hole, we placed a slime mould (10mm  $\varnothing$ ) in the centre of the arena  
307 2cm away from each food. We replicated the experiment 50 times for each food quality. For each  
308 replicate, we measured the time taken by the slime mould to reach either one of the three food  
309 sources.

310 To assess the difference in the latency to reach the food as a function of the food quality, we  
311 used a linear mixed model (function `lmer`, Package `lme4`) in R (RStudio Version 1.2.1335). The  
312 models were fitted by specifying the fixed effects (explanatory variables) the concentration in yolk  
313 (continuous predictor). The sclerotia identity was also added to the model as a random factor. We  
314 transformed the dependant variable using the “bestNormalize” function (“bestNormalize” package).  
315 The outcome of the model is presented in the supplementary information (Table S2).

### 316 **Optimal policies**

317 Optimal policy computations were performed in Matlab (*MathWorks, 2020*), and were adapted  
318 from the dynamic program of *Tajima et al. (2019)*. Optimal policies were computed for Bayes Risk  
319 and geometric discounting, for linear utility ( $r := x$ ), and for non-linear utility functions having the  
320 form

$$r := m \left( \frac{1}{1 + e^{-sx}} - 1 \right) \quad (1)$$

321 where  $m$  and  $s$  are shape parameters for the logistic function determining the interval of utilities  
322 and steepness of the slope respectively, and  $x$  is the raw input value. We systematically varied the  
323  $m$  and  $s$  parameters to test magnitude-sensitivity under Bayes Risk optimisation and geometric  
324 discounting, under a range of utility function shapes ranging from almost linear, to almost stepwise.  
325 Note that a sigmoid curve includes an interval in which subjective utility is an accelerating function  
326 of input value when the latter is negative, and an interval in which it is a decelerating function when  
327 the latter is positive; thus testing for magnitude-sensitivity over the full interval of raw input values  
328 tests a variety of utility function shapes over sub-intervals.

329 The Bellman equation used in the dynamic programming analysis for the Bayes Risk-optimisation  
330 case was

$$V(t, \hat{\mathbf{x}}(t)) = \max \{ \max_i \{ r_i(t, \hat{\mathbf{x}}(t)) \} - \rho t_w, \langle V(t + \delta t, \hat{\mathbf{x}}(t + \delta t)) \rangle - (c + \rho)\delta t \}, \quad (2)$$

331 where  $V(t, \hat{\mathbf{x}}(t))$  is the value of the state estimates vector  $\hat{\mathbf{x}}(t)$  at time  $t$ ,  $r_i(t, \hat{\mathbf{x}}(t))$  is similarly the  
332 expected reward from choosing the  $i$ -th reward,  $\delta t$  is the time interval to the next decision point,  $c$   
333 is the linear cost per unit time,  $\rho$  is the reward rate per unit time based on optimal decision-making  
334 over a sequence of trials,  $t_w$  is the inter-trial waiting time, and  $\langle \dots \rangle$  is expectation over the next time  
335 interval ( $\delta t$ ) (*Tajima et al., 2019*). For the results presented here we set  $c = 0$ ,  $t_w = 1$  and found the  
336 optimal  $\rho > 0$  using the methods of *Tajima et al. (2019)*; note, however, that since the prior was not  
337 varied this reward-rate optimisation could not induce magnitude-sensitive reaction times in itself.

338 For the geometric discounting case the Bellman equation becomes

$$V(t, \hat{\mathbf{x}}(t)) = \max \{ \max_i \{ r_i(t, \hat{\mathbf{x}}(t)) \}, \langle V(t + \delta t, \hat{\mathbf{x}}(t + \delta t)) \rangle^\gamma \}, \quad (3)$$

339 where  $0 < \gamma < 1$  is a discount factor for rewards received in future timesteps; this discount factor is  
340 per-unit-time, hence to discount a reward  $\delta t < 1$  timesteps in the future the appropriate factor is  
341  $\gamma^{\delta t/1} = \gamma^{\delta t}$ .

### 342 Stochastic simulations

343 Since noise processing is important in determining reaction times, we derived optimal decision  
344 policies as above, then tested them through numerical analysis of stochastic models. To test for  
345 magnitude-sensitive decision-making we examined the case of  $n = 3$  equal-quality alternatives, in  
346 which we varied the magnitude of the (equal) stimuli values. Through these stochastic simulations,  
347 we tested the impact of the different temporal discount methods—linear or geometric—and of  
348 different utility functions—linear or nonlinear—on the decision speed (reaction time RT). The  
349 stochastic models simulate the sequential accumulation of evidence for the three alternatives  
350  $i \in \{1, 2, 3\}$  that are used to compute the expected rewards  $\langle \hat{x}_i(t) \rangle$ . The three evidence estimates  
351 can be represented, with a little abuse of notation, as a vector  $\hat{\mathbf{x}}(t)$  denoting a point in a cube that  
352 represents the estimate space. In that cube, we also include the decision boundaries computed  
353 as above, indicating the separation of the estimate space into decision regions; in one region  
354 continuing to sample is expected to maximise utility, and in the other region taking a decision for  
355 the leading option is expected to be the best action.

356 In our simulations, each time step of length  $dt$  the decision-maker accumulates three pieces of  
357 evidence, one for each option. Evidence for an option  $i$  is sampled from the normal distribution  
358  $\mathbf{X}_i \sim \mathcal{N}(\bar{x}_i dt, \sigma_{a,i}^2 dt)$ , where each sample  $x_{\tau,i}$  is a piece of momentary evidence at a small timestep  
359 of length  $dt$  and with sequential index  $\tau$ ,  $\bar{x}_i$  is the true raw value (before any nonlinear utility  
360 transformation) of option  $i$  and  $\sigma_{a,i}^2$  is the variance in accumulation of evidence for  $i$  (**Tajima et al.,**  
361 **2016**). Before observing any evidence, the decision maker has prior mean and variance,  $\bar{x}_{p,i}$  and  
362  $\sigma_{p,i}^2$  for the distribution of  $\mathbf{X}_i$ . Each new piece of accumulated evidence is used by the decision  
363 maker to update the posterior expected reward as

$$\langle \hat{x}_i(t) \rangle = \frac{\bar{x}_{p,i} \sigma_{a,i}^2 + \sum_{\tau=1}^t dx_{\tau,i}}{\sigma_{a,i}^2 + \sigma_{p,i}^2 t}. \quad (4)$$

### 364 Code and Data Availability

365 Optimisation codes for the results presented here can be downloaded from

366 <https://github.com/DiODEProject/MultiAlternativeDecisions/tree/stochastic-sim>

367 Experimental code and data for the results presented here can be downloaded from

368 <https://osf.io/8jumk/>

## 369 Acknowledgements

370 We thank Satoshi Tajima for sharing the code for the binary decision model. Dr Tajima was an  
371 exceptionally promising scientist who is sadly missed. We thank Jan Drugowitsch and Alex Pouget  
372 for discussions of their results and our own, and Thomas Bose, Nathan Lepora and Sophie Baker  
373 for comments on an earlier draft.

## 374 Declaration of Conflicting Interests

375 The authors declare that they have no conflicting interests.

## 376 References

- 377 Bhui, R. (2019). Testing optimal timing in value-linked decision making. *Computational Brain & Behavior*, 2(2):85–  
378 94.
- 379 Bogacz, R., Brown, E., Moehlis, J., Holmes, P., and Cohen, J. D. (2006). The physics of optimal decision making:  
380 a formal analysis of models of performance in two-alternative forced-choice tasks. *Psychological Review*,  
381 113(4):700.
- 382 Dussutour, A., Ma, Q., and Sumpter, D. (2019). Phenotypic variability predicts decision accuracy in unicellular  
383 organisms. *Proceedings of the Royal Society B*, 286(1896):20182825.
- 384 Fawcett, T. W., Fallenstein, B., Higginson, A. D., Houston, A. I., Mallpress, D. E., Trimmer, P. C., and McNamara, J. M.  
385 (2014). The evolution of decision rules in complex environments. *Trends in Cognitive Sciences*, 18(3):153–161.
- 386 Fudenberg, D., Strack, P., and Strzalecki, T. (2018). Speed, accuracy, and the optimal timing of choices. *American*  
387 *Economic Review*, 108(12):3651–84.
- 388 Houston, A. I. and McNamara, J. M. (1999). *Models of adaptive behaviour: an approach based on state*. Cambridge  
389 University Press.
- 390 Krajbich, I., Armel, C., and Rangel, A. (2010). Visual fixations and the computation and comparison of value in  
391 simple choice. *Nature neuroscience*, 13(10):1292–1298.
- 392 Latty, T. and Beekman, M. (2011). Speed–accuracy trade-offs during foraging decisions in the acellular slime  
393 mould *Physarum polycephalum*. *Proceedings of the Royal Society B: Biological Sciences*, 278(1705):539–545.
- 394 Mangel, M. and Clark, C. W. (1988). *Dynamic modeling in behavioral ecology*. Princeton University Press.
- 395 Marshall, J. A. R. (2019). Comment on ‘optimal policy for multi-alternative decisions’. *bioRxiv*.
- 396 MathWorks (2020). Matlab r2020b.
- 397 McNamara, J. M. and Houston, A. I. (2009). Integrating function and mechanism. *Trends in Ecology & Evolution*,  
398 24(12):670–675.
- 399 Pais, D., Hogan, P. M., Schlegel, T., Franks, N. R., Leonard, N. E., and Marshall, J. A. R. (2013). A mechanism for  
400 value-sensitive decision-making. *PLoS one*, 8(9):e73216.
- 401 Parker, G. A. and Smith, J. M. (1990). Optimality theory in evolutionary biology. *Nature*, 348(6296):27.



- 402 Peirce, J., Gray, J. R., Simpson, S., MacAskill, M., Höchenberger, R., Sogo, H., Kastman, E., and Lindeløv, J. K. (2019).  
403     Psychopy2: Experiments in behavior made easy. *Behavior research methods*, 51(1):195–203.
- 404 Peirce, J. W. (2007). Psychopy—psychophysics software in python. *Journal of neuroscience methods*, 162(1-2):8–13.
- 405 Pirrone, A., Azab, H., Hayden, B. Y., Stafford, T., and Marshall, J. A. (2018a). Evidence for the speed–value trade-off:  
406     Human and monkey decision making is magnitude sensitive. *Decision*, 5(2):129.
- 407 Pirrone, A. and Gobet, F. (2021). Is attentional discounting in value-based decision making magnitude sensitive?  
408     *Journal of Cognitive Psychology*.
- 409 Pirrone, A., Stafford, T., and Marshall, J. A. R. (2014). When natural selection should optimize speed-accuracy  
410     trade-offs. *Frontiers in neuroscience*, 8:73.
- 411 Pirrone, A., Wen, W., and Li, S. (2018b). Single-trial dynamics explain magnitude sensitive decision making. *BMC*  
412     *neuroscience*, 19(1):1–10.
- 413 Reid, C. R., MacDonald, H., Mann, R. P., Marshall, J. A., Latty, T., and Garnier, S. (2016). Decision-making without  
414     a brain: how an amoeboid organism solves the two-armed bandit. *Journal of The Royal Society Interface*,  
415     13(119):20160030.
- 416 Sellitto, M., Ciaramelli, E., and di Pellegrino, G. (2010). Myopic discounting of future rewards after medial  
417     orbitofrontal damage in humans. *Journal of Neuroscience*, 30(49):16429–16436.
- 418 Smith, S. M. and Krajbich, I. (2019). Gaze amplifies value in decision making. *Psychological Science*, 30(1):116–128.
- 419 Steverson, K., Chung, H.-K., Zimmermann, J., Louie, K., and Glimcher, P. (2019). Sensitivity of reaction time to the  
420     magnitude of rewards reveals the cost-structure of time. *Scientific Reports*, 9(1):1–14.
- 421 Tajima, S., Drugowitsch, J., Patel, N., and Pouget, A. (2019). Optimal policy for multi-alternative decisions. *Nature*  
422     *Neuroscience*, 22:1503–1511.
- 423 Tajima, S., Drugowitsch, J., and Pouget, A. (2016). Optimal policy for value-based decision-making. *Nature*  
424     *Communications*, 7:12400.
- 425 Teodorescu, A. R., Moran, R., and Usher, M. (2016). Absolutely relative or relatively absolute: violations of value  
426     invariance in human decision making. *Psychonomic Bulletin & Review*, 23(1):22–38.
- 427 Turner, W., Feuerriegel, D., Andrejevic, M., Hester, R., and Bode, S. (2019). Perceptual change-of-mind decisions  
428     are sensitive to absolute evidence magnitude. *PsyArXiv*.
- 429 Zajkowski, W., Krzemiński, D., Barone, J., Evans, L., and Zhang, J. (2019). Reward certainty and preference bias  
430     selectively shape voluntary decisions. *bioRxiv*, page 832311.